Vol 13 No 8, August 2004
1009-1963/2004/13(08)/1239-07

Chinese Physics

© 2004 Chin. Phys. Soc.
and IOP Publishing Ltd

Production of helium projectile fragments in ^{16}O–emulsion interactions at 4.5 A GeV/c*

Zhang Dong-Hai(张东海), Li Zhen-Yu(李振宇),
Li Jun-Sheng(李俊生), and Wu Feng-Juan(吴凤娟)

Institute of Modern Physics, Shanxi Teachers' University, Linfen 041004, *China*

(Received 27 October 2003; revised manuscript received 25 April 2004)

The measurements of partial production cross sections of the multiple helium projectile fragments emitted at 4.5 A GeV/c ^{16}O–Em interactions are reported. We have studied the production rate of helium projectile fragments due to fragmentation of ^{16}O ions and compared it with that obtained from different projectiles at various energies. The dependence of $< n_\alpha >$ on the mass number of the incident beams is formulated. The multiplicity distributions of the helium fragments produced in ^{16}O–Em interactions at different energies exhibit Koba–Nielson–Olesen (KNO) scaling. The correlation of helium projectile fragments and target fragments is also investigated and it is found that the average of target fragments is increased with the decrease of the number of helium fragments in peripheral interactions.

Keywords: relativistic heavy-ion collision, helium projectile fragments, KNO scaling, production cross-section, multiplicity correlation

PACC: 2570N, 2587

1. Introduction

Heavy ion collisions at high energies have been attracting more and more interest in recent years due to the developments at the accelerator facilities at CERN Super Proton Synchrotron (SPS), the Lawrence Berkeley Radiation Laboratory (LBL) Bevalac, the Brookhaven National Laboratory (BNL) Alternating Gradient Synchrotron (AGS) and Relativistic Heavy Ions Collider (RHIC), and the Joint Institute of Nuclear Research (JINR) Dubna synchrophasotron. The main objective of heavy ion collisions is to observe the signatures of unusual forms of nuclear matter such as the quark–gluon plasma which may be produced in collisions at relativistic energies. However, an interesting domain of physics can also be studied in peripheral collisions involving heavy ion beams. A study of secondary helium projectile fragments (HPFs) produced in high-energy heavy ion collisions has been regarded as a potentially useful source of information about the underlying production processes. Consequently, helium emission in heavy ion reactions was carefully studied from different points of view even before the 1990s.[1−11] In these researches, significant conclusions have been acquired on the fragmentation of nuclei into multiple helium fragments. In the last ten years, the projectile helium fragments produced from various heavy ion beams at different energies have been studied exclusively,[12−18] and it was observed that the multiplicity distributions of alpha fragments obey a universal scaling and that the transverse momenta distributions can be explained by two or three different emission sources at different temperatures.

The detection of HPFs in nuclear research emulsion is quite definite because of their distinctive grain density. The use of NIKFI BR-2 nuclear emulsion detectors in the present experiment allows an exclusive-type analysis on an event by event basis. The emulsion detector is very suitable for studies of nucleus–nucleus reactions because it registers all charged particles of an individual event in a 4π-geometry due to its high spatial resolution.

In the present work, we present and discuss experimental data on some of the characteristics of HPFs produced by collisions of ^{16}O nucleus with nuclear emulsion at 4.5 A GeV/c. The multiplicity scaling

*Project supported by the National Natural Science Foundation of China (Grant No 10275042), the Shanxi Provincial Natural Science Foundation (Grant No.20021007) and Shanxi Provincial Foundation for Returned Scholars of China.

of HPFs and the correlation of HPFs and target fragments are investigated. The Koba–Nielson–Olesen[19] (known as KNO) scaling hypothesis has become a dominant framework to study the behaviour of the multiplicity distributions of hadron–hadron collisions, Jain *et al*[7,10] studied the validity of that scaling in nucleus–nucleus interactions at CERN and Berkeley energies. The present work is a continuation of our previous work of the production of HPFs in ^{16}O–emulsion collisions at 60 A GeV.[20] We intend to check whether our previous work about the HPF scaling can be extended to the Dubna energy. We also want to see how the production of HPFs changes with projectile energy.

2. Experimental details

NIKFI BR-2 stacks of nuclear emulsions, 10cm× 10cm×2cm in volume, were exposed horizontally to the 4.5 A GeV/c ^{16}O beam at Synchrophasotron of the JINR, Dubna. The flux intensity was 10^3particles/cm^2. Emulsion plates, 600μm in thickness, were scanned by the along-the-track method using XSJ-1 and XSJ-2 microscopes under 100× oil objectives and 16× eyepieces. The tracks were picked up at a distance of 1cm from the edge of the pellicle and were carefully followed until they either interacted with the nuclei of the emulsion or escaped from the pellicle. Details about scanning and measurements have been given elsewhere.[21,22] A total of 2292 interactions of oxygen with the nuclei of the emulsion were observed by following 28390.4cm of primary track length, leading to a mean free path $\lambda = (12.39 \pm 0.26)$cm. Among these interactions, 111 events were found to be produced by electromagnetic interactions and 109 events were due to elastic interactions. Out of these 2292 interactions, 1239 were picked up, without any bias, for the final analysis. Interactions which were within 30μm from the top or bottom surface of the emulsion were not considered for the final analysis.

The tracks of the emitted secondary charged particles in each interaction were classified, in accordance with the emulsion terminology, into the following types:

(a) Shower tracks $N_{\rm s}$ correspond to the produced single-charged relativistic particles having a velocity $\beta \geq 0.7$. Most of these tracks belong to pions contaminated by a small proportions of fast protons and K mesons. Their multiplicity is denoted by $n_{\rm s}$ (not including the stripped projectile protons).

(b) Grey tracks $N_{\rm g}$, with a range in emulsion $L >$ 3mm and velocity $0.3 < \beta < 0.7$, are produced mostly by recoil protons in the kinetic energy range $26 \leq E \leq 375$MeV and a few kaons of kinetic energies $20 \leq E \leq 198$MeV and pions with kinetic energies of $12 \leq E \leq 56$MeV. The corresponding multiplicity of these grey tracks is denoted by $n_{\rm g}$.

(c) Black tracks $N_{\rm b}$, with a range in emulsion $L \leq$ 3mm and $\beta < 0.3$, correspond to protons with kinetic energies $E \leq 26$MeV, produced by low-energy target fragments. Their multiplicity is denoted by $n_{\rm b}$.

The grey and black tracks together are called heavy ionizing particles. Their multiplicity is denoted by $n_{\rm h} = n_{\rm g} + n_{\rm b}$.

(d) Projectile fragments $N_{\rm f}$, charged particles emitted at an angle (relative to the beam direction) $\theta \leq \Theta_{\rm f}$ ($\Theta_{\rm f}$ is the projectile fragmentation angle), without change in its ionization for at least 2cm from the interaction point, is considered as a noninteracting projectile fragment. The fragmentation angle is defined as $\Theta_{\rm f} = p_{\rm f}/p_{\rm beam}$, where $p_{\rm beam}$ stands for the beam momentum and $p_{\rm f}$ for the Fermi momentum of nucleon; the latter is estimated to be 200 MeV/c, thus giving $\Theta_{\rm f} \approx 45$mrad for present incident energy. The charges of all the projectile fragments ($Z \geq 3$) were identified by the delta-ray-counting method.

Each event was carefully examined and qualitatively classified into three principal categories, depending upon the following visual characteristics:

(1) Near-central events: events which exhibit no visible forward-cone fragments of charge $Z \geq 2$ from the projectile. Such events are thought to be created by violent destruction of the projectile and target nuclei at small values of the impact parameter b of the collision.

(2) Semi-central or peripheral events: events with projectile fragments (PFs) of charge $Z \geq 2$ emitted in a forward cone. These events show considerably less involvement of the projectile nucleus since they are formed at relatively large values of b.

(3) Electromagnetic events: events generated by the electromagnetic dissociation (ED) of the incident nuclei which are generated in collisions involving impact parameters large enough so that no nuclear interaction occurs and extremely strong electromagnetic fields from heavy target nuclei are produced for a very short time. Such events typically consist of PFs, which proceed in the direction of the projectile nucleus and are confined within an angle of 45mrad to the beam direction.

3. Experimental results

Out of 1239 inelastic interactions, 550 events having at least one HPF produced in ^{16}O–emulsion interactions have been investigated in the present work. A total of 881 HPFs have been selected in these 550 peripheral inelastic events.

3.1. Partial production cross-section

Table 1 shows the partial cross sections for central σ_c, peripheral σ_p and multiple helium $\sigma_{n\alpha}$ events. For comparison, the corresponding values for 60[10,20] and 200 A GeV[10] ^{16}O are also given in this table. The values of σ_α can be obtained using the relation

$$\sigma_{n\alpha} = \sigma_{\rm inel} \frac{\text{Number of events having } n\alpha}{\text{Total number of interactions}}, \quad (1)$$

where $\sigma_{\rm inel}$ is the total experimental reaction cross section of the present beam which is found to be 898 ± 20mb.

Table 1. Partial production cross sections for different reaction channels.

Reaction channel	Cross section(mb)			
	200 A GeV[10] G5 emulsion	60 A GeV[10] G5 emulsion	60 A GeV[20] BR2 emulsion	3.7 A GeV BR2 emulsion
Central collision	348 ± 33	301 ± 24	294 ± 18	304 ± 15
Peripheral collision	754 ± 49	690 ± 37	632 ± 19	594 ± 21
$n\alpha$ Channel	406 ± 36	369 ± 27	404 ± 15	390 ± 17
0α Channel	348 ± 33	321 ± 25	228 ± 11	204 ± 12
1α Channel	238 ± 28	201 ± 20	225 ± 11	217 ± 13
2α Channel	103 ± 18	102 ± 14	127 ± 8	112 ± 9
3α Channel	61 ± 14	66 ± 11	50 ± 5	56 ± 6
4α Channel			4 ± 1	5 ± 2

Table 2. The percentage of α-multiplicity for different projectiles at various energies.

Beam	1α	2α	3α	4α	4,5,6α's	Ref.
2.1 A GeV ^{16}O	43.5 ± 3.4	32.7 ± 3.0	21.6 ± 2.4	2.2 ± 0.8		[11]
3.7 A GeV ^{16}O	56.4 ± 3.2	28.4 ± 2.3	13.9 ± 1.6	1.3 ± 0.5		This work
14.6 A GeV ^{16}O	47.4 ± 5.2	34.7 ± 4.5	17.3 ± 3.2	0.6 ± 0.6		[11
60 A GeV ^{16}O	47.3 ± 6.1	27.1 ± 4.6	22.8 ± 4.2	3.1 ± 1.6		[11]
60 A GeV ^{16}O	55.4 ± 2.8	31.3 ± 2.1	12.3 ± 1.3	1.0 ± 0.4		[20]
60 A GeV ^{16}O	54.6 ± 5.4	27.6 ± 3.9	17.8 ± 3.1			[10]
200 A GeV ^{16}O	59.2 ± 6.9	25.6 ± 4.5	15.2 ± 3.5			[10]
200 A GeV ^{16}O	49.0 ± 3.5	32.2 ± 2.9	17.5 ± 2.1	1.3 ± 0.6		[11]
3.7 A GeV ^{12}C	61.1	28.9	10.1			[23]
3.7 A GeV ^{22}Ne	60.0	24.3	11.6	3.5	3.7	[23]
3.7 A GeV ^{24}Mg	52.8	26.1	13.4	7.0	7.7	[24]
3.7 A GeV ^{28}Si	47.5	30.6	14.1		7.8	[23]
3.7 A GeV ^{28}Si	50.0	29.3	14.4	4.1	6.2	[25]

It is noted that the partial production cross sections for all reaction channels of ^{16}O at 3.7, 60 and 200 A GeV are close to each other. Also, the production cross sections for channels with different α, which are approximately the same within experimental errors, confirm the fact that the interaction cross section does not depend on the projectile incident energy in the nucleus–nucleus interaction. This conclusion confirms the limiting fragmentation hypothesis.

Table 2 gives the percentages of α-particle multiplicity productions for ^{16}O–Em interaction at different energies and for different projectile-induced nuclear emulsion interaction at the same energy (3.7 A GeV). It should be noted that the percentage of α multiplicities seems to be constant and independent of the incident beam and energy. The percentage for producing 1α is about two times that for 2α and three times that for 3α. For heavier beams the production of 4αs, 5αs and 6αs constitutes about 6%–9% of the total number of events having α-fragments.

3.2. Scaling of the multiplicity distributions of HPFs

It is reported in recent papers[7,10,12,18,26] that the validity of the KNO[19] scaling holds for the HPFs produced in heavy ion collisions at Dubna, Bevatron, CERN and AGS energies. Here we discuss the multiplicity distribution of HPFs produced in ^{16}O–Em interaction at 4.5 A GeV/c. KNO scaling hypothesis was originally derived by assuming Feynman scaling of the inclusive particle production cross section. This states that the multiplicity distributions of the form

$$\Psi(Z) =< n_\alpha > \sigma_{n_\alpha}/\sigma_{\rm inel} \qquad (2)$$

should be an asymptotical energy-independent function of $Z = n_\alpha / < n_\alpha >$, where n_α refers to the number of HPFs in an event and $< n_\alpha >$ is the average HPF multiplicity. σ_{n_α} is the partial cross section for producing a state of multiplicity n_α and $\sigma_{\rm inel}$ is the total inelastic cross section.

The multiplicity of the produced HPFs from the events of different projectiles over a wide range of energies can be represented by a universal function of the following form:

$$\Psi(Z) = AZ\exp(-BZ), \qquad (3)$$

where A and B are constants.

In Fig.1 we plot $< n_\alpha > \sigma_{n_\alpha}/\sigma_{\rm inel}$ as a function of the scaled $n_\alpha / < n_\alpha >$ for HPFs produced in ^{16}O–Em interactions at 3.7 A GeV compared with those for ^{16}O at 60, and 200 A GeV. In spite of a wide difference in energy scale, the data points lie on the same scaling curve, suggesting a universal behaviour of the helium multiplicity distributions. The simple functional form expressed by Eq.(3) with two adjustable parameters A and B is again seen to provide a good description of the multiplicity distributions over the entire energy range. For the present experiment, $A = 3.30 \pm 0.27$ and $B = 2.56 \pm 0.06$ with χ^2/dof=0.28, where dof means degree of freedom. The approximate stability of the multiplicity distributions for HPFs over a wide range of incident energies and projectile masses has no obvious physical explanation and can perhaps be usefully interpreted as an empirical observation for the time being.

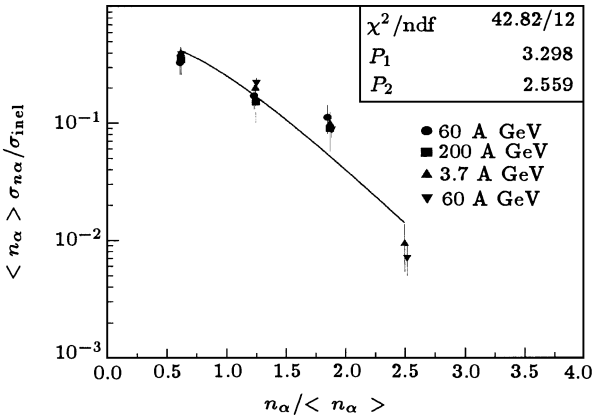


Fig.1. The multiplicity distribution $< n_\alpha > \sigma_{n_\alpha}/\sigma_{\rm inel}$ versus $n_\alpha / < n_\alpha >$ for HPFs. The curve is obtained by fitting the data by Eq.(3).

Table 3. The mean values of α-particle production, moments C_q and the second Muller moment f_2 for different projectiles at various energies.

Beam	$< n_\alpha >$	C_2	C_3	C_4	C_5	f_2	Ref.
3.7 A GeV ^{16}O	$1.60 \pm .05$	$1.23 \pm .07$	$1.81 \pm .16$	$2.99 \pm .35$	$5.38 \pm .78$	1.0 ± 0.1	Ours
14.6 A GeV ^{16}O	1.7 ± 0.1	1.2 ± 0.1	1.7 ± 0.1	2.6 ± 0.2	4.3 ± 0.1	1.1 ± 0.1	[11]
60 A GeV ^{16}O	1.7 ± 0.1	1.2 ± 0.1	1.7 ± 0.1	2.8 ± 0.1	4.7 ± 0.2	1.1 ± 0.1	[11]
60 A GeV ^{16}O	$1.59 \pm .03$	$1.21 \pm .01$	$1.74 \pm .01$	$2.82 \pm .01$	$4.96 \pm .02$	1.1 ± 0.1	[20]
60 A GeV ^{16}O	$1.62 \pm .10$	$1.23 \pm .01$	$1.77 \pm .11$	$2.85 \pm .17$	$4.88 \pm .29$	1.0 ± 0.1	[10]
200 A GeV ^{16}O	$1.60 \pm .15$	$1.22 \pm .11$	$1.74 \pm .16$	$2.76 \pm .26$	$4.64 \pm .43$	1.0 ± 0.1	[10]
200 A GeV ^{16}O	1.7 ± 0.1	1.2 ± 0.1	1.7 ± 0.1	2.6 ± 0.1	4.3 ± 0.2	1.1 ± 0.1	[11]
3.7 A GeV ^{12}C	1.5 ± 0.1	1.2 ± 0.1	1.7 ± 0.2	2.7 ± 0.2	4.7 ± 0.4	1.0 ± 0.1	[23]
3.7 A GeV ^{22}Ne	1.6 ± 0.1	1.3 ± 0.1	2.1 ± 0.1	4.0 ± 0.1	8.5 ± 0.2	0.9 ± 0.1	[23]
3.7 A GeV ^{24}Mg	1.8 ± 0.1	1.3 ± 0.1	2.1 ± 0.1	3.9 ± 0.2	7.9 ± 0.5	0.8 ± 0.1	[24]
3.7 A GeV ^{28}Si	1.9 ± 0.1	1.3 ± 0.1	2.2 ± 0.1	4.4 ± 0.2	8.9 ± 0.3	0.8 ± 0.1	[23]
3.7 A GeV ^{28}Si	1.8 ± 0.1	1.3 ± 0.1	2.1 ± 0.1	4.2 ± 0.1	9.3 ± 0.3	0.8 ± 0.1	[25]

Another consequence of the multiplicity scaling implies the energy-independent moments given by

$$C_q =< n^q > / < n >^q =< Z^q >= \int Z^q \Psi(Z) {\rm d}Z. \quad (4)$$

For KNO scaling to hold the C_q moments should be energy-independent. Consequently, in Table 3 we present the experimental values of the average multiplicities and the C_q moments for q=2, 3, 4, 5 of

the Z=2 secondaries from interactions of ^{16}O in emulsion at different incident energies and also ^{12}C, ^{22}Ne, ^{24}Mg and ^{28}Si at the same incident energy (3.7 A GeV). It is obvious from this table that the values of moments C_q do not seem to depend upon the energy for the same projectile beam within the experimental errors. On the other hand, the moments C_2 do not change with projectile energy and mass, the higher moments indicate a slow increase with the projectile mass number. The second Muller moments, $f_2 = (C_2 - 1) < n_\alpha >^2 - < n_\alpha >$, are nonzero. This shows a strong correlation among the produced HPFs. The variation of the average multiplicity $< n_\alpha >$ with A (projectile mass) is shown in Fig.2. The increase of $< n_\alpha >$ with A can be approximately parametrized by the formula

$$< n_\alpha >= k_1 A^{k_2}, \qquad (5)$$

where $k_1 = 0.474 \pm 0.039$ and $k_2 = 0.417 \pm 0.019$ in this experiment with χ^2/dof=0.418. The values of k_1 and k_2 are approximately consistent with those of Ref.[10]. A point worth noting is that the mean HPF multiplicity is independent of the incident energy for the same projectile (see for example ^{16}O, $< n_\alpha > \approx 1.6$ despite of large difference in beam energy).

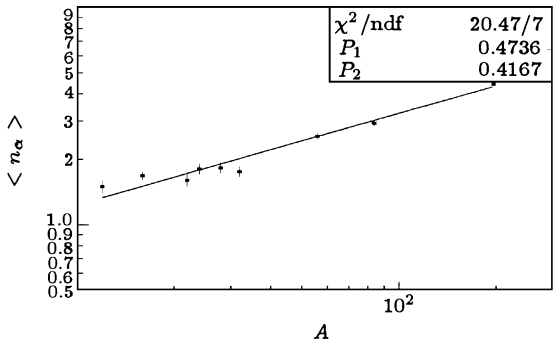


Fig.2. Dependence of $< n_\alpha >$ with A. The curve is a fit to the data. The functional form employed is given in Eq.(5) in the text.

3.3. Correlation between target fragments and HPFs

The characteristic features of nucleus–nucleus interactions at relativistic energies depend, from the geometrical point of view, on the impact parameter. The type of interaction is determined by the value of impact parameter $|(R_T - R_P)| < b \leq (R_T + R_P)$ for peripheral and semi-central interactions, and $0 \leq b \leq |(R_T - R_P)|$ for central interactions, where R_T and R_P is the radius of the target nucleus and projectile, respectively. In peripheral interactions the colliding nuclei are well separated in their centres. This allows only a small momentum transfer between the nuclei, leading to the break-up of one or both of them into fragments. The characteristics of the emitted fragments are determined by the intrinsic Fermi momentum distributions of nucleons within the fragmenting nuclei. Based on the colliding geometry, the participant–spectator model is given to describe the features of the relativistic nucleus–nucleus interactions in which nucleons residing in the geometrical overlap between projectile and target are considered to be participants of the heavy ion collision, whereas the nucleons not residing in the overlap are termed spectators. Spectators from projectile decay through evaporation of neutrons and light nuclei for low excitation energy or disintegrates into fragments of intermediate mass at higher excitation energies, forming the projectile fragments. Spectators from target decay through evaporation to form target fragments. The production of HPFs which come from the projectile spectator is strongly correlated with the production of target fragments. In the central collisions, projectile and target completely overlap (for $R_T > R_P$), projectile spectator is zero and the excitation of target spectator is the highest and so the mean value of target fragments is the largest. In the semi-central and peripheral collisions, the projectile spectator increases with the increase of the impact parameter b, and so the production probability of the HPFs increases, but the excitation of the target spectator decreases with the increase of b and so the average multiplicity of target fragments decreases.

Figure 3 shows the target multiplicity distributions for different α-channels with N_f=0 and $N_f \geq 0$, where N_f is the number of projectile fragments with charge $Z \geq 3$ in an event. It is shown that N_h distributions change most strongly with the increase in the number of HPFs for both cases (N_f=0 and $N_f \geq$0): their broadness changes their shape substantially. The width of the distribution decreases with the increase of the number of HPFs for both cases. The contribution from small values of N_h for N_f=0 is greater than that for $N_f \geq$0 for cases with N_α=0, 1 and 2, but for cases with N_α=3 and 4 the distributions are the same.

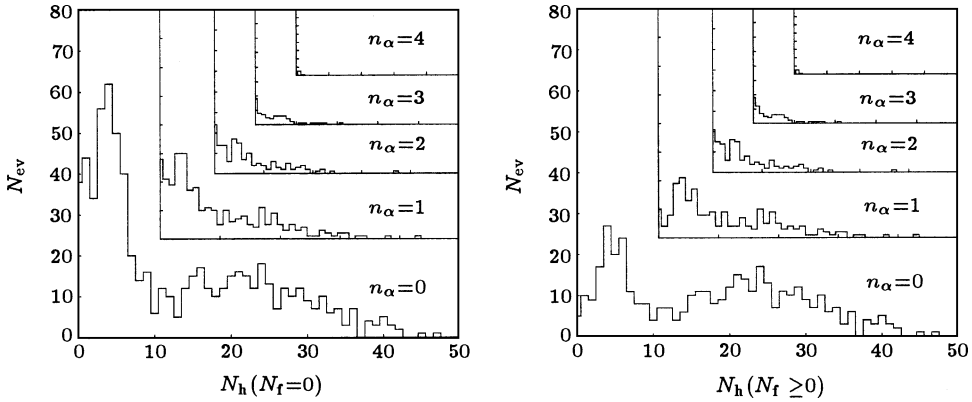


Fig.3. The multiplicity distributions of target fragments for different α channels.

Table 4. Dependence of N_h and n_α for different N_f.

n_α	$< N_h >$		
	N_f=0	N_f >0	$N_f \geq$0
0	17.48 ± 0.87	5.27 ± 0.31	12.47 ± 0.47
1	10.89 ± 0.75	3.63 ± 0.37	8.60 ± 0.49
2	6.41 ± 0.53	4.10 ± 1.30	6.26 ± 0.50
3	4.17 ± 0.48	—	4.17 ± 0.48
4	1.00 ± 0.38	—	1.00 ± 0.38

Figure 4 and Table 4 show the correlation between the mean multiplicity of target fragments $< N_h >$ and the number of HPFs for N_f=0 and $N_f \geq$0. It is shown from the figure that $< N_h >$ depends linearly on the number of HPFs apart from the case of N_α=0 (central collision). The $< N_h >$ value decreases with the increase of the number of HPFs for both cases. The dependence of $< N_h >$ on the number of HPFs can be described by the following linear relation for semi-central and peripheral collisions:

$$< N_h >= a + bn_\alpha. \quad (6)$$

By using minimum χ^2 fitting, we obtain $a = 13.42 \pm 0.63$, $b = -3.11 \pm 0.12$ with χ^2/dof=0.09 for the N_f=0 case and $a = 11.43 \pm 0.54$, $b = -2.59 \pm 0.16$ with χ^2/dof=0.30 for $N_f \geq$0. The number of HPFs, similar to N_h, can be regarded as a quantitative measure of the impact centrality.

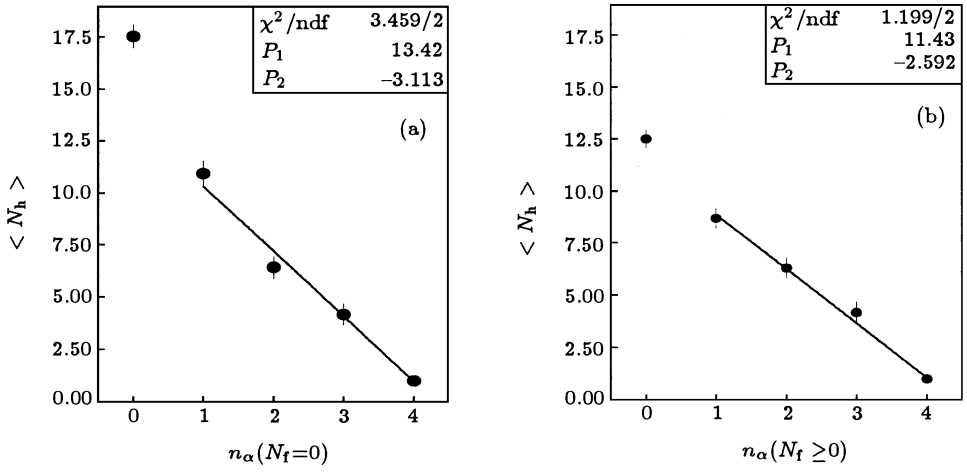


Fig.4. The mean multiplicity of target fragments $< N_h >$ versus n_α.

We have also studied the correlation between $< n_\alpha >$ and N_h, as shown in Fig.5. From the figure it is seen that the mean value of HPFs deceases with the increase of the number of target fragments. The maximum production probabilities of HPFs are at N_h=0 and 1, which correspond to ^{16}O-H interactions and the peripheral collision of ^{16}O–Em.

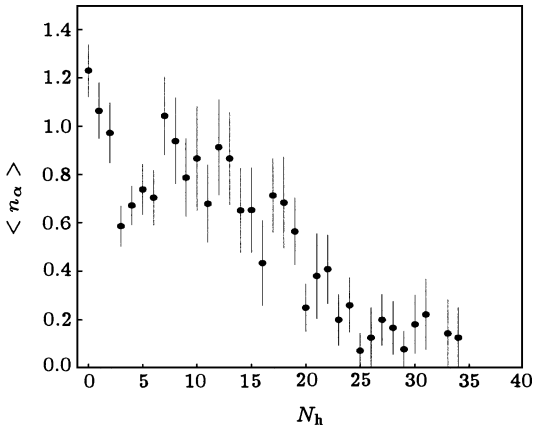


Fig.5. The mean multiplicity of HPFs $< n_\alpha >$ versus N_h.

4. Conclusion

From the analysis of 1239 ^{16}O–Em interactions at 4.5 A GeV/c we can conclude:

1. The multiplicity distributions of the HPFs produced in ^{16}O at 3.7, 60 and 200 A GeV exhibit a KNO scaling. The values of moments C_q ($q = 2 - 5$) are found to be independent of the energies for the same projectile (^{16}O). The value of moment C_2 is independent of the mass and energy of the projectile, the higher moments indicate a slow increase with the mass of the projectile.

2. The average multiplicity $< n_\alpha >$ for different projectiles at various incident energies can be parametrized in terms of the projectile mass A(Eq.5).

3. There are strong correlations between the production of target fragments and the HPFs. The mean multiplicity of the target fragments decreases with the increase of the number of the HPFs, and also the average multiplicity of the HPFs decreases with the increase of the number of the target fragments.

Acknowledgment

We are thankful to Professor I. Otterlund at Lund University in Sweden for supplying the emulsion plates.

References

[1] Baumgart H G *et al* 1975 *Z. Phys. Rev.* A **237** 359
[2] Jakobsson B *et al* 1977 *Nucl. Phys.* A **276** 523
[3] Goldhaber A S 1974 *Phys. Lett.* B **53** 306
[4] Greiner D E *et al* 1975 *Phys. Rev. Lett.* **35** 152
[5] Gosset J *et al* 1977 *Phys. Rev.* C **16** 629
[6] Aggarwal M M *et al* 1983 *Phys. Rev.* C **27** 640
[7] Jain P L and Aggarwal M M 1986 *Phys. Rev.* C **33** 1790
[8] Singh G, Sengupta K and Jain P L 1988 *Phys. Lett.* B **214** 480
[9] Joseph R R *et al* 1989 *J. Phys.* G **15** 1805
[10] Sengupta K, Singh G and Jain P L 1989 *Phys. Lett.* B **222** 301
[11] Adamovich M I *et al* (EMU-01 Collaboration) 1989 *Phys. Rev.* C **40** 66
[12] El-Nadi M *et al* 1993 *Int. J. Mod. Phys.* E **2** 381
[13] Adamovich M I *et al* (EMU-01 Collaboration) 1994 *Phys. Lett.* B **338** 397
[14] Singh G and Jain P L 1994 *Z. Phys.* A **348** 99
[15] Cherry M L, Dabrowska A and Deines-Jones P 1997 *Z. Phys.* C **73** 449
[16] Adamovich M I *et al* (EMU-01 Collaboration) 1997 *Phys. Lett.* B **390** 445
[17] Kamel S 1999 *Nuovo Cimento* A **112** 733
[18] El-Nadi M, El-Nagdy M S and Ali-Mossa N 2002 *J. Phys.* G **28** 1251
[19] Koba Z, Nielson B and Olesen P 1972 *Nucl. Phys.* B **40** 317
[20] Zhang D H 2002 *High Energy Phys. Nucl. Phys.* **26** 40 (in Chinese)
[21] Zhang D H, Sun H C and Gharibi G 2001 *Chin. Phys.* **10** 21
[22] Zhang D H 2002 *Chin. Phys.* **11** 1254
[23] El-Nadi M *et al* 1993 *Int. J. Mod. Phys.* **2** 381
[24] El-Nadi M *et al* 1995 *Nuovo Cimento* A **108** 935
[25] Singh B K, Ojha I D and Tuli S K 1994 *Nucl. Phys.* A **570** 819
[26] Singh G, Ismail A Z M and Jain P L 1991 *Phys. Rev.* C **43** 2417